Hänsch TW, Picqué N. Frequency combs. In: Träger F, editor. Handbook of lasers and optics. 2nd ed. Springer Berlin: Heidelberg; (2012).

Ideguchi T et al. Adaptive real-time dual comb spectroscopy. arXiv:1201.4177 (2012).

Jacquet, P., et al. Frequency comb Fourier transform spectroscopy with kHz optical resolution. In: Fourier transform spectroscopy. Washington, DC: Optical Society of America; 2009. paper FMB2, 3 p.

Keilmann F, Gohle C, Holzwarth R. Time-domain mid-infrared frequency-comb spectrometer. Opt Lett. 2004;29:1542–4.

Kippenberg TJ, Holzwarth R, Diddams SA. Microresonator-based optical frequency combs. Science. 2011;332(6029):555–9.

Mandon J, Guelachvili G, Picqué N. Fourier transform spectroscopy with a laser frequency comb. Nat Photonics. 2009; 3:99–102.

Schliesser A, et al. Frequency-comb infrared spectrometer for rapid, remote chemical sensing. Opt Express. 2005; 13(22):9029–38.

Thorpe MJ, et al. Broadband cavity ringdown spectroscopy for sensitive and rapid molecular detection. Science. 2006;311:1595–9.

Udem T, Holzwarth R, Hänsch TW. Optical frequency metrology. Nature. 2002;416:233–7.

Wang CY et al. Mid-infrared frequency combs based on microresonators. arXiv:1109.2716 (2011).

Yasui T, Saneyoshi E, Araki T. Asynchronous optical sampling terahertz time-domain spectroscopy for ultrahigh spectral resolution and rapid data acquisition. Appl Phys Lett. 2005;87:061101.

Optical Trap

Optical Tweezers

Ximiao Hou and Wei Cheng
Department of Pharmaceutical Sciences, University of Michigan, Ann Arbor, MI, USA

Synonyms

Bacterial flagellar motor: biophysical studies; Laser trap; Optical trap; Single-molecule methods

Definition

Optical tweezers are focused laser beams that can trap and manipulate microscopic objects contact-free in three dimensions (3D).

Introduction

Photons carry momentum and can therefore exert forces on matter. Although the typical force generated by photons is very small, the range of force (10^{-12} N, pN) is significant for microscopic objects and macromolecules at the nanometer scale. Optical tweezers exploit this fundamental property to trap micron-sized objects in a potential well formed by light and allow manipulation of these objects in 3D. More importantly, optical tweezers can be used as quantitative tools to directly measure force and displacement once they are coupled with sensitive measurements of light. Since the first demonstration of stable optical trapping of micron-sized dielectric objects by Ashkin and coworkers (Ashkin et al. 1986), optical tweezers have found increasing use in biophysical investigations. The continued development of optical tweezers over the years has made them a highly sensitive and quantitative tool in biophysics to manipulate and measure macromolecular interactions, one molecule at a time.

Principles of Optical Trapping

An optical trap is formed by focusing a laser beam to a diffraction-limited spot with a high Numerical Aperture (NA) objective. As photons carry momentum, a dielectric object situated in the light path will experience a force that pushes the object in the direction of light propagation due to scattering of photons by the object. At the same time, the electric field of the light wave induces transient dipoles in the dielectric object. The interactions between these transient dipoles and the electric field give rise to a force that aligns in the direction of the field gradient. When the laser beam is focused through an objective, the direction of the field gradient points toward the focus of the laser beam where the laser beam has the highest intensity. This gradient force is proportional to both the electric field gradient and the polarizability of the

dielectric object, and counteracts the scattering force so that the particle can be stably trapped in 3D very close to the laser focus.

To understand the interaction between light and a dielectric particle quantitatively, microscopic objects have been classified into three regimes based on their size:

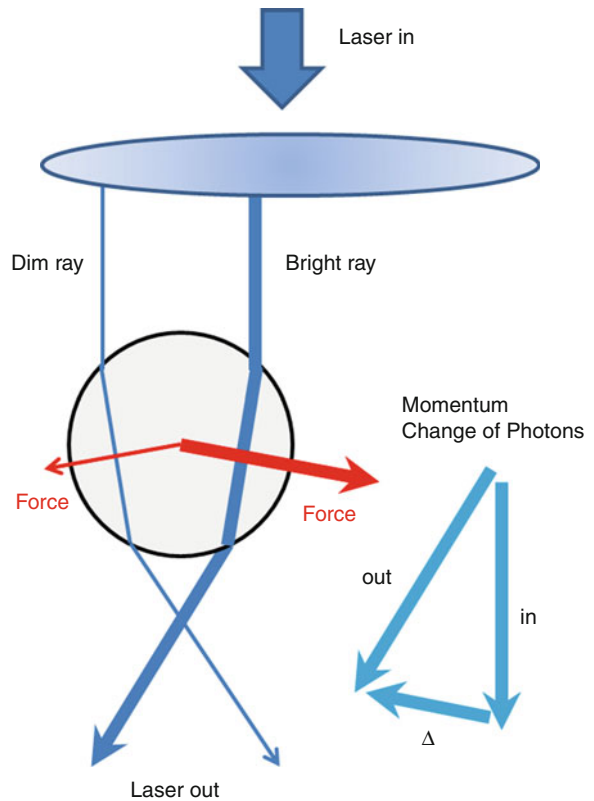### Particle Diameter $>>$ Laser Wavelength λ

In this regime, ray optics can well describe the origin of trapping forces. As shown in Fig. 1, a laser beam of Gaussian intensity profile is focused through a positive lens, and a bead is located downstream of the focused beam slightly off the optical axis. Consider the bright ray on the right that propagates through the bead, it will change its direction upon exiting the bead due to refraction. Because the refractive index of the bead is higher than that of the surrounding media, the exiting ray will point away from the optical axis. This net change in photon momentum suggests that the bead exerts a force on the laser beam in the direction of the momentum change. According to Newton's third Law, the bead will experience a reacting force of the same magnitude but in opposite direction, exerted by the photons (indicated by the red thick arrow). The same analysis applies to the dim ray on the left. As a result, there is a net force acting on the bead that points toward the focus of the laser beam, which gives rise to the trapping force. Conversely, if the bead has a lower refractive index than the surrounding media, it will be pushed away from the laser focus instead of being stably trapped.

Rayleigh Particle: Diameter $<< \lambda$

In this regime, ray optics no longer applies. The interaction of the particle with photons can be approximated by the interaction of a transient dipole with the electromagnetic wave of the light. The scattering force, as described above, is proportional to the scattering cross section of the particle and can be calculated as follows (Harada and Asakura 1996):

$$\vec{F}_{\text{scat}} = \frac{\bar{z}n_2}{c} \frac{8\pi(ka)^4a^2}{3} \left(\frac{m^2-1}{m^2+2}\right)^2 I \quad (1)$$

where $\bar{z}$ is the unit vector in the beam-propagation direction, n_2 is the refraction index of the surrounding medium, m is the effective index n_1/n_2, where n_1 is the refraction index of the particle, a is the particle diameter, k is the wave number $2\pi/\lambda$, where λ is the laser wavelength, and I is the beam intensity.


Optical Tweezers, Fig. 1 Basic principle for optical tweezers to trap a particle in the ray optics regime (particle diameter d $>>$ laser wavelength λ). Incident laser beam is assumed to have a Gaussian intensity profile, as indicated by the *gradient color* shaded along the positive lens. Light rays of higher intensity are noted using *thicker blue lines*

The gradient force can be calculated from the time average of the Lorentz force exerted on the transient dipole by the electromagnetic field as follows:

$$\vec{F}_{\text{grad}} = \left\langle [\vec{P} \cdot \nabla] \vec{E} \right\rangle_{\text{T}} = \frac{2\pi n_2 a^3}{c} \left(\frac{m^2-1}{m^2+2}\right) \nabla I \quad (2)$$

where $\vec{P}$ is the dipole moment, $\vec{E}$ is the instantaneous electric field, and c is the speed of light in vacuum. As shown in (2), the direction of the gradient force aligns with the direction of the beam intensity gradient.

The majority of microscopic objects used in optical trapping have a size range that is comparable to the wavelength of the trapping light. The exact theoretical treatment is much more complex, and simple analytical solutions for scattering and gradient forces are not yet available.
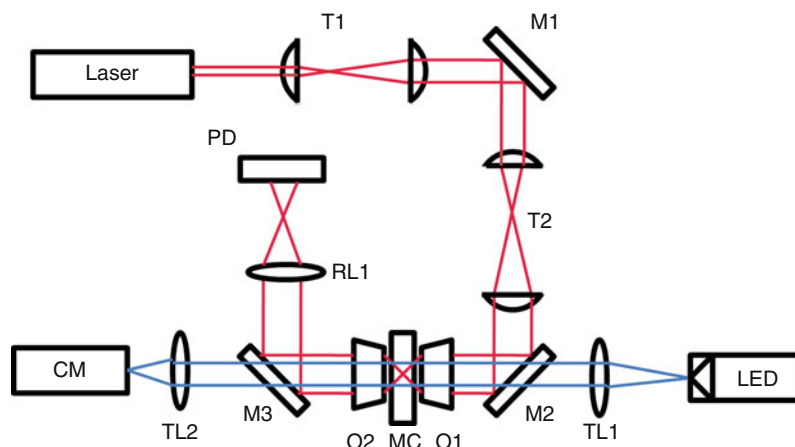
Optical Tweezers, Fig. 2 A schematic of an optical tweezers setup. A laser beam is expanded by a telescope (T1). It is then deflected by a mirror (M1) and sent through a second telescope (T2) to further expand the beam. After this final beam expansion and deflection by a dichroic mirror (M2), the objective O1 focuses the beam to a diffraction-limited spot to form an optical trap at the center of a microfluidic chamber (MC). A second objective (O2) is used to collect the light exiting from the optical trap. The exiting beam is deflected by a third mirror M3 and projected onto a photodetector (PD) through a relay lens (RL1). A light-emitting diode (LED) is installed to provide the bright field illumination (*blue lines*) for the MC. The image of the MC is projected onto a CCD camera (CM) through a tube lens (TL2)
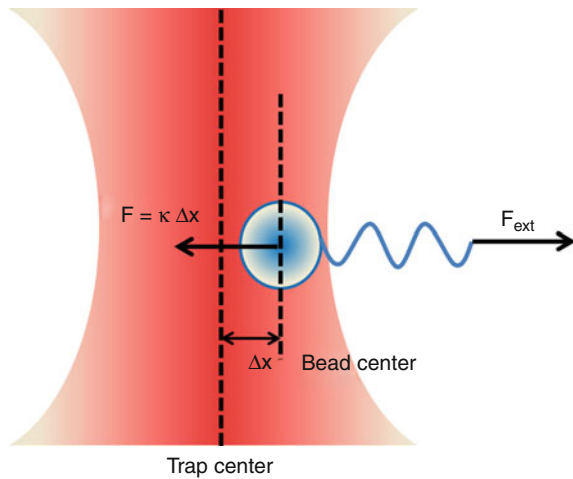
Optical Tweezers Setup

Figure 2 is a schematic diagram of a single-beam gradient optical tweezers setup. It contains the following essential components: a laser to provide the light source for forming the optical trap, a telescope to expand the laser beam to overfill the back aperture of an objective (O1) to make the trap strong, and the front objective (O1) to focus the laser beam to form the optical trap. For quantitative detection and measurement of optical tweezers, a back objective (O2) is typically used to collect light exiting from the optical trap and a photodetector (PD) is used for quantitative measurement of the light. Building on this basic concept of optical trapping, more complex optical tweezers can be designed and constructed. For example, a dual-trap optical tweezers can be constructed by splitting the single beam using a polarizing beam splitter to produce two orthogonally polarized beams. Alternatively, multiple optical traps can be created by either time-sharing of a single laser beam through the use of acousto-optic deflectors (AOD) (Dame et al. 2006) or splitting of a single beam by diffraction optical elements (DOE) to form arrays of optical tweezers, named "holographic optical tweezers (HOT)" (Dufresne and Grier 1998). In addition, the wavelength of the laser should be carefully selected because photochemical effects have been demonstrated for certain wavelengths, which is especially important for biological applications.

Displacement Detection

Lateral motion of a trapped object at the sample plane will produce a laser intensity shift at the back focal plane of the objective O2, which arises from the interference between the forward scattered light and the unscattered light that differ by $90°$ in their phases. When the movement of the object is small compared to the radius of the beam focus, this spatial shift in laser intensity is proportional to the displacement of the trapped object away from its equilibrium position and, therefore, can be used to measure the lateral displacement of the object. In practice, a position-sensitive photodetector is placed at a location that is conjugate to the back focal plane of the objective O2. By monitoring the laser intensity shift on the photodetector, lateral position of the trapped particle can be determined with nanometer precision (Gittes and Schmidt 1998a).

Optical Tweezers, Fig. 3 Optical tweezers behave as a Hookean spring
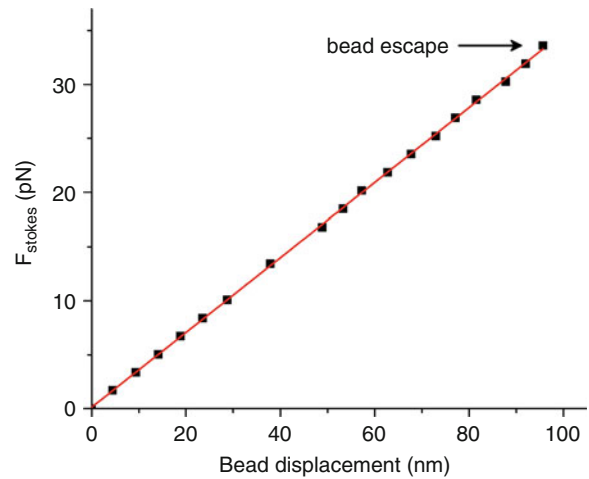
Optical Tweezers, Fig. 4 The Stokes force experienced by a bead in an optical trap was determined using Stokes' Law. The displacement of the bead in the optical trap was measured using video microscopy. The slope of the curve defines the stiffness of the optical trap

Force Measurement

A particle in an optical trap experiences a restoring force when there is a displacement. The value of the force is proportional to the displacement, i.e., an optical trap behaves as a Hookean spring to the trapped particle with a spring constant k (Fig. 3):

$$\vec{F} = -k\vec{x} \qquad (3)$$

where $\vec{x}$ is the vectorial displacement of the particle. When k is known, the force can be calculated accordingly. The spring constant of the trap (also called stiffness) is dependent on a number of parameters that include laser power, numerical aperture of the objective, particle size, and its refractive index (Simmons et al. 1996). Stiffness values of 0.005–1 pN/nm have been reported throughout the literature.

Measurement of Trap Stiffness

Numerous methods have been developed in the literature to measure the stiffness of an optical trap. Among these, two methods have been frequently used.

1. *Calibration using viscous drag of a fluid*. Trap stiffness can be derived by applying an external viscous drag force on the bead and measuring its displacement. This is typically achieved through applying a laminar flow to the solution, where the particle is being trapped. For a solution of viscosity η that flows at a rate of v, the viscous drag experienced by a trapped spherical particle of radius r can be determined by Stokes' Law:

$$\mathrm{F_{stokes}} = 6\pi\eta\mathrm{r}v \qquad (4)$$

By adjusting the flow rate, a series of forces $\mathrm{F_{stokes}}$ can be applied and the resulting displacement x of the bead be measured. Trap stiffness can be derived simply from the slope of the $\mathrm{F_{stokes}}$-x curve (Fig. 4).

When the viscous drag force exceeds the maximum force that the trap can exert on the bead, the bead will no longer stay in the trap but move together with the flow. The force at which this occurs is termed trap "escape force", which can be measured by increasing the flow speed until the bead is carried away by the flow. Typically, the trap escape force increases linearly with laser power (Simmons et al. 1996).

2. *Calibration by Brownian motion*. The stiffness of an optical trap can also be obtained by measuring the Brownian motion of a trapped bead. A trapped bead undergoes damped Brownian motions, and its movement in solution is governed by three forces: the random thermal force F(t), the trap restoring force kx, and the viscous drag force γdx/dt, where γ is the drag
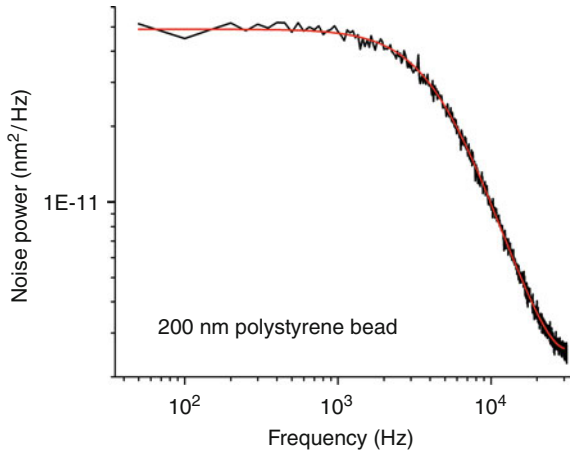
Optical Tweezers, Fig. 5 Power spectrum of a trapped bead. The corner frequency can be estimated by fitting the power spectrum with (6)

coefficient and dx/dt is the instantaneous velocity. The Langevin equation for such a system can be written as follows:

$$\gamma \frac{d\vec{x}}{dt} + k\vec{x} = \vec{F}(t) \qquad (5)$$

The power spectrum of the bead position $S_x(f)$ can be derived by applying a Fourier transformation to both sides of (5) (Gittes and Schmidt 1998b) and is defined as follows:

$$S_x(f) = \frac{k_B T}{\gamma \pi^2 \left(f_c^2 + f^2\right)} \qquad (6)$$

where k_B is the Boltzmann constant, T is the absolute temperature, and f_c defines the corner frequency of the trap as $f_c = k/2\pi\gamma$.

Figure 5 shows a typical power spectrum of a trapped bead, which can be divided into two regimes: when $f << f_c$, the power spectrum is almost constant; when $f >> f_c$, the power spectrum instead decreases with a rate of $1/f^2$. Once the value of f_c is found, the stiffness can be determined with $k = 2\pi\gamma f_c$, where γ can be calculated as $\gamma = 6\pi\eta r$ for a bead with known radius r in a medium with viscosity η. A more complex equation for the bead Brownian motion power spectrum has been derived to correct for nonideal conditions, for example, finite sampling and friction in an incompressible fluid (Berg-Sorensen and Flyvbjerg 2004).

Applications of Optical Tweezers

Since the invention of optical tweezers by Ashkin and coworkers, this contact-free manipulation technique has found broad applications in physics, chemistry, and biology. Optical tweezers can be used to manipulate and position small objects such as viruses, bacteria, eukaryotic cells, as well as cellular organelles. With optical tweezers, single cells or micron-sized particles can be positioned, transported, and even sorted (MacDonald et al. 2003).

The remarkable features of optical tweezers to directly apply and measure mechanical force in the piconewton range have been employed to study the mechanical properties of cell membranes. For example, a red blood cell was stretched through two attached beads by optical tweezers, and large deformations were captured under various applied forces. The membrane shear modulus can thus be measured using this technique.

Coupled with sensitive measurement of light, optical tweezers have become an important tool to study the biochemical and biophysical properties of motor proteins and biopolymers at the single-molecule level. To manipulate these single molecules using optical tweezers, micron-sized beads are usually used as mechanical handles: molecules are attached to a bead through complementary biochemistry, and then manipulated and measured through the bead. Three major types of single-molecule experiments have been developed. Type one is a surface-based experiment. As shown in Fig. 6a, one end of a single-molecule tether is attached to a bead that is held in an optical trap, while the other end of the molecule attaches to a substrate surface. This scheme has been used to follow cytoskeleton motor proteins and nucleic acids motor proteins. The disadvantage of this experimental geometry is stage drift that is independent of the laser trap, which has to be subtracted to reach high spatial resolution (Carter et al. 2009). Type two is a pipette-based experiment. As shown in Fig. 6b, one end of a single-molecule tether is attached to a bead held by an optical trap while the other end is attached to a bead held on top of a micropipette. This type of experiment can be carried out deep in solution, and thus potential concerns from being close to a surface are eliminated. Still, noise arises from the drift of the micropipette that is independent of the optical trap. Type three is a dual-beam optical tweezers. As shown
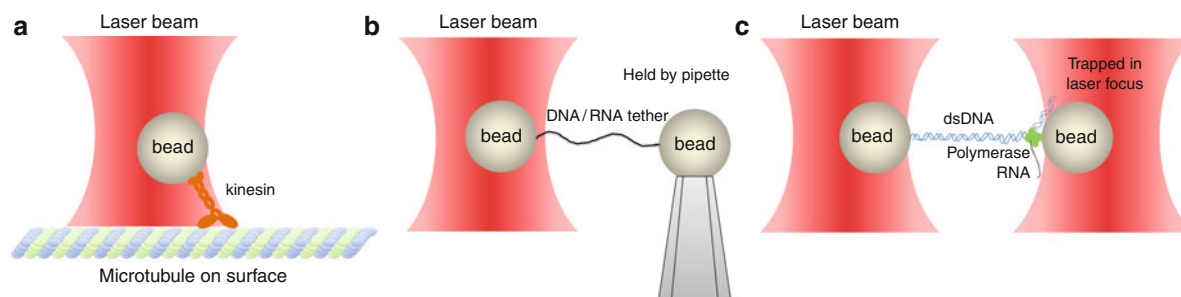
Optical Tweezers, Fig. 6 Schematics of single-molecule optical tweezers experiments

in Fig. 6c, two traps are formed from a single laser beam split by polarization. Because the entire molecule is optically levitated in solution, stage drift becomes a minimal concern (Abbondanzieri et al. 2005). In addition, as these two traps are formed using the same beam source, noise of common origins, for example, beam-pointing instability can be effectively canceled out by conducting measurements along a difference coordinate (Moffitt et al. 2006). These developments have pushed the spatial resolution of optical tweezers to the subnanometer regime.

Different single-molecule systems have been studied using the experimental schemes described above. These systems range from molecular motors to single biopolymers.

Molecular motors. Optical tweezers have been widely used to track the movement of motor proteins, including cytoskeleton motor protein families and nucleic acid translocases. One of the best studied cytoskeleton motor proteins is kinesin. Kinesins move on microtubules and are important for cargo transport inside the cell. One experimental scheme is to attach the motor protein to a micron-sized bead that is trapped by optical tweezers with high precision (Fig. 6a). Block and coworkers measured the step size of Kinesin to be 8 nm (Svoboda et al. 1993), which offered one of the first examples that biological motors move with regular steps. This result agrees well with the 8 nm spacing of each tubulin dimer. A unique feature of optical tweezers is the ability to measure the opposing force at which the motor will stop its movement. The stall force of a single kinesin was measured to be 7 pN (Visscher et al. 1999). Myosin, on the other hand, has an average step size of 11 nm and stall forces of 3–5 pN (Finer et al. 1994).

The broad families of nucleic acid translocases have been studied using optical tweezers (Bustamante et al. 2011). They include DNA and RNA polymerases, helicases, DNA packaging motors, ribosomes, and many other nucleic acids translocases. Although these proteins carry out different biological functions inside the cell, the common property they share is the ability to move on DNA or RNA molecules. High-resolution optical tweezers enable real-time observations of single motor-protein activity. The important questions that can be addressed include the velocity of movement, translocation step size, processivity, conformational dynamics, and physical mechanisms that underlie the basis of movement. For example, Bustamante and coworkers carried out systematic studies on the DNA packaging motor of bacteriophage φ29 (Bustamante et al. 2011). The velocity, stall force, step size of the motor, and potential mechanisms of force generation by the motor, and its interaction with DNA have all been quantified using optical tweezers. Block and coworkers used dual-beam optical tweezers with subnanometer spatial resolution to measure the step size of RNA polymerase (RNAP), using the experimental design schematically shown in Fig. 6c (Abbondanzieri et al. 2005). RNAP transcription changes the extension of the DNA in between the two beads, and the step size of RNAP was measured to be one base pair at a time. Many other nucleic acids motors such as DNA polymerases, DNA or RNA helicases have also been studied by optical tweezers. With the development of optical tweezers down to the subnanometer resolution regime, more exciting discoveries on motor movement are expected.

Elasticity of nucleic acids. Elasticity is an important property of biopolymers. The elasticity of double-stranded DNA (dsDNA) directly affects the physiological states of DNA such as wrapping around histones, loop formation, and DNA packaging. As a quantitative tool for single-molecule manipulation, optical tweezers have been used to measure the force-extension curves of

double- as well as single-stranded DNA (ssDNA), from which important parameters such as persistence length can be extracted. One of the pioneering works in this area was carried out by Bustamante and coworkers (Smith et al. 1996) using the design shown in Fig. 6b. Single DNA molecule was stretched by moving the pipette away from the laser focus. The end-to-end extension of the DNA and the force on the molecule were measured. The persistence length of dsDNA was determined to be 193 bp in 150 mM NaCl solution. Interestingly, when the force is increased to 65 pN, the molecule undergoes a sudden cooperative transition in which the extension of the DNA is lengthened to 1.7 times that of a standard B-DNA form. The exact nature of this transition is a matter of ongoing research. Binding of DNA by proteins or intercalating ligands changes the interphosphate distance or the persistence length of the molecule and, thus, changes the force-extension curve of dsDNA. Optical tweezers have become a powerful tool to study DNA-binding proteins and intercalating ligands, shedding light on the mechanism of protein or ligand action.

Single-molecule folding and unfolding. Optical tweezers are a facile tool to study folding and unfolding of proteins or nucleic acids. The reaction coordinate of a folding/unfolding transition is well defined when a single protein molecule or nucleic acid is held on its two extremities and force is applied to induce the structural transition. Extensive studies of this kind have been performed on RNA structures (Tinoco et al. 2006) and model proteins (Cecconi et al. 2005). The force at which these molecules unfold, the pathway of folding and unfolding, and the distance to the transition state can all be mapped or measured using optical tweezers. In addition, a characteristic hopping phenomenon unique to single-molecule observations was revealed when the molecule was held at a tension close to the mechanical unfolding force.

Summary

The invention of optical tweezers together with the development of this technique over the years have brought about many interesting and exciting discoveries in biophysics that were not possible to achieve before. Optical tweezers are a unique tool that allows biophysicist to study force, displacement generated by single biomolecules, and probe the inner working of a molecule at unprecedented scale and resolution.

Compared to ▶ magnetic tweezers, optical tweezers can provide higher spatial resolution (0.1–2 nm) and higher force (200 pN). In addition, clever use of nonspherical particles or nanofabricated quartz cylinders allows one to apply ▶ torque with optical tweezers (Deufel et al. 2007). Compared to the ▶ atomic force microscope (AFM), which can supply higher forces (10^4 pN), optical tweezers offer higher spatial resolution with lower stiffness. The unique capability of optical tweezers to manipulate microscopic objects, apply and measure mechanical force, and quantify displacement at subnanometer resolution will continue to offer much excitement in biophysics. Notably, optical tweezers also expand their ability through a combination with ▶ single-molecule fluorescence technique. Using this hybrid technique, one can not only manipulate and measure molecules as described above, but can also image the molecules simultaneously through a fluorescence signal from dye labels. Combined with microfluidic techniques, researchers can control and trigger biochemical reactions while manipulating single molecules. The development of these hybrid techniques along with laser trapping will continue to make optical tweezers a powerful and precise tool in biophysical research.

Cross-References

▶ Angular Optical Trapping
▶ Atomic Force Spectroscopy
▶ Bacterial Flagellar Motor: Biophysical Studies
▶ Dual-Beam Optical Tweezers
▶ Force-Fluorescence Spectroscopy
▶ Laser Processing of Biomaterials and Cells
▶ Magnetic Tweezers
▶ Microfluidics for Single Molecule Detection

References

Abbondanzieri EA, Greenleaf WJ, Shaevitz JW, Landick R, Block SM. Direct observation of base-pair stepping by RNA polymerase. Nature. 2005;438:460–5.

Ashkin A, Dziedzic J, Bjorkholm J, Chu S. First demonstration of stable optical trapping of micron-sized dielectric objects in three dimensions using a single-beam gradient optical trap. Opt Lett. 1986;11:288–90.

Berg-Sorensen K, Flyvbjerg H. Power spectrum analysis for optical tweezers. Rev Sci Instrum. 2004;75:594–612.

Bustamante C, Cheng W, Meija YX. Revisiting the central dogma one molecule at a time. Cell. 2011;144:480–97.

Carter AR, Seol Y, Perkins TT. Precision surface-coupled optical-trapping assay with one-basepair resolution. Biophys J. 2009;96:2926–34.

Cecconi C, Shank EA, Bustamante C, Marqusee S. Direct observation of the three-state folding of a single protein molecule. Science. 2005;309:2057–60.

Dame RT, Noom MC, Wuite GJL. Bacterial chromatin organization by H-NS protein unravelled using dual DNA manipulation. Nature. 2006;444:387–90.

Deufel C, Forth S, Simmons CR, Dejgosha S, Wang MD. Nanofabricated quartz cylinders for angular trapping: DNA supercoiling torque detection. Nat Methods. 2007;4:223–5.

Dufresne ER, Grier DG. Optical tweezer arrays and optical substrates created with diffractive optics. Rev Sci Instrum. 1998;69:1974–7.

Finer JT, Simmons RM, Spudich JA. Single myosin molecule mechanics: piconewton forces and nanometre steps. Nature. 1994;368:113–9.

Gittes F, Schmidt CF. Interference model for back-focal-plane displacement detection in optical tweezers. Opt Lett. 1998a;23:7–9.

Gittes F, Schmidt CF. Signals and noise in micromechanical measurements. Methods Cell Biol. 1998b;55:129–56.

Harada Y, Asakura T. Radiation forces on a dielectric sphere in the Rayleigh scattering regime. Opt Commun. 1996;124:529–41.

MacDonald MP, Spalding GC, Dholakia K. Microfluidic sorting in an optical lattice. Nature. 2003;426:421–4.

Moffitt JR, Chemla YR, Izhaky D, Bustamante C. Differential detection of dual traps improves the spatial resolution of optical tweezers. Proc Natl Acad Sci USA. 2006;103:9006–11.

Simmons RM, Finer JT, Chu S, Spudich JA. Quantitative measurements of force and displacement using an optical trap. Biophys J. 1996;70:1813–22.

Smith SB, Cui Y, Bustamante C. Overstretching B-DNA: the elastic response of individual double-stranded and single-stranded DNA molecules. Science. 1996;271:795–9.

Svoboda K, Schmidt CF, Schnapp BJ, Block SM. Direct observation of kinesin stepping by optical trapping interferometry. Nature. 1993;365:721–7.

Tinoco Jr I, Li PT, Bustamante C. Determination of thermodynamics and kinetics of RNA reactions by force. Q Rev Biophys. 2006;39:325–60.

Visscher K, Schnitzer MJ, Block SM. Single kinesin molecules studied with a molecular force clamp. Nature. 1999;400:184–9.

Optoacoustic Spectroscopy

▶ Fourier Transform Infrared Photoacoustic Spectroscopy (FTIR-PAS)

ORC1 Human Ornithine Carrier Isoform 1

▶ Mitochondrial Transport Protein Family: Structure

ORC1, ORC2 Mitochondrial Ornithine Carriers

▶ Mitochondrial Transport Protein Family

ORC2 Human Ornithine Carrier Isoform 2

▶ Mitochondrial Transport Protein Family: Structure

Order of Reaction

Clive R. Bagshaw
Department of Biochemistry, University of Leicester, Leicester, UK
Department of Chemistry and Biochemistry, University of California Santa Cruz, Santa Cruz, CA, USA

Definition

The Order of Reaction refers to the power dependence of the rate on the concentration of each reactant. Thus, for a first-order reaction, the rate is dependent on the concentration of a single species. A second-order reaction refers to one whose rate is dependent on the square of the concentration of a single reactant (e.g., in a homo-dimerization reaction, $A + A \rightarrow A_2$) or the combined first-order dependence on the concentrations of two different reactants ($A + B \rightarrow C$). The order of reaction is an experimentally determined parameter and can take on a fractional value. This is distinct from the *molecularity* (or stoichiometry) of the reaction which is the theoretical integer value of the number of molecules involved in the reaction. For simple one-step reactions, the *order* and *molecularity* should have the same value. A classic example of fractional order is the simple enzyme scheme under steady-state conditions; $E + S \leftrightarrow ES \rightarrow E + P$. Here, the rate of production of product P is first order with respect to E and first order with respect to S at low concentrations of S. At high concentrations of S the reaction becomes limited by the second step which shows first-order dependence on E but zero order with respect to S. At intermediate concentrations of S the reaction will show between zero- and first-order dependence on [S].